TABLE 2

Clinical findings of patients 1, 2, and 26 with rare molecular defects.

		Patient 1	Patient 2		Patient 26	
Molecular defects						
Mutation		*FGFR1* deletion	*SOX3* mutation		*WDR11* mutation	
Parental origin of mutation		Unknown	Unknown		Mother	
Clinical features						
Diagnosis		nIHH	nIHH		CPHD	
Genital abnormality at birth		Cryptorchidism (left)[a]	None		None	
Defective sex development		Micropenis/small testis (at 13.2 y)	Small testis, no pubertal development (at 16 y)		Micropenis (at 7.0 y)	
Other clinical feature		None	Short stature		Short stature,[b] obesity, MR	
Olfactory function		Normal	Normal		Normal	
Brain MRI		Normal	Hypoplastic anterior pituitary		Pituitary malformation[c]	
Endocrine data (age at exam.)	Stimulant[d]	13.2	10.9	16.9, 18.3[e]	1.7, 2.3, 3.5[f]	7.0
LH (IU/L)	GnRH	**0.1→ 1.7**	**<0.1→** 6.4	**<0.1→ 3.6**		**<0.2→ 0.2**
FSH (IU/L)	GnRH	0.3→ 3.2	2.4→ 16.2	0.5→ 4.8		<0.5→ 2.0
T (nmol/L)	hCG	0.1→ 0.1	0.6			
GH (ng/mL)	Insulin	1.16→ 10.10	0.60→ **1.50**			
GH (ng/mL)	Arginine				→ **1.42**[g]	
GH (ng/mL)	Clonidine		1.30→ 9.81		→ **0.62**[g]	
GH (ng/mL)	L-dopa		0.30→ 18.78			
IGF-I (ng/mL)		151	178	222	→ **<4**[g]	
TSH (mIU/L)	TRH	1.2→ 12.7	1.2		3.2	2.3→ 10.4
Free T_4 (pmol/L)		0.18	0.17		0.17	0.15
ACTH (pg/mL)	Insulin/CRH[h]	13.1→ 393.0	67.8		20.1 → 57.3	11.0→ 28.7
Cortisol (μg/dL)	Insulin/CRH[h]	3.1→ 29.1	23.6		10.0→ 20.9	7.0→ 20.8
PRL (ng/mL)	TRH	3.5→ 55.2	6.1			4.0→ **4.9**

Note: Hormone values below the age- and sex-matched reference range are bold-faced. Hormone levels are shown as (basal values)→ (peak values). CPHD = combined pituitary hormone deficiency; CRH = corticotropin- releasing hormone; fT4 = free thyroxine; IGF1 = Insulin- like growth factor 1; MR = mental retardation; T = testosterone; TRH = thyrotropin releasing hormone; nIHH = normosmic isolated hypogonadotropic hypogonadism.

[a] Subjected to orchiopexy at 2 years of age.

[b] Treated with GH from 1.9 years of age.

[c] Stalk interruption and ectopic posterior lobe.

[d] GnRH (100 μg/m^2), insulin (0.1 U/kg), arginine (0.5 g/kg), TRH (10 μg/kg), and CRH (1.5 μg/kg) IV; clonidine (0.1 mg/m^2) and L-DOPA (10 mg/kg) orally; blood sampling at 0, 30, 60, 90, and 120 minutes. In CRH stimulation test, additional blood sampling was performed at 15 minutes. hCG (3,000 U). IM for 3 consecutive days; blood sampling on days 1 and 4.

[e] LH and FSH were measured at 16.9 years of age and IGF-I was measured at 18.3 of age.

[f] GH and IGF-I were measured at 1.7 years of age, ACTH and cortisol were measured at 2.3 years of age, and other hormones were measured at 3.5 years of age.

[g] Basal values were not available.

[h] Insulin and CRH were used for patients 1 and 26, respectively.

Izumi. Genetic basis of gonadotropin deficiency. Fertil Steril 2014.

first polyalanine tract in SOX3. *SOX3* encodes a transcription factor involved in pituitary morphogenesis (13). Duplications and deletions of alanine residues in *SOX3* have been shown to cause various types of pituitary dysfunction in male and, less frequently, in female subjects (14, 16). Our data broaden the phenotypic variation of polyalanine deletions in *SOX3* to include nIHH. Patient 26 carried a hitherto unreported mutation of *WDR11* that probably disrupts the protein structure of WDR11 by causing exon skipping. WDR11 has recently been shown to play a role in the development of hypothalamic neurons (34). Five missense mutations in *WDR11* have been identified in six patients with nIHH/KS (12). Our results indicate that *WDR11* mutations can underlie not only nIHH/KS but also CPHD. Because previous studies revealed that nIHH, KS, and CPHD are genetically related conditions resulting from defective formation of the anterior midline in the forebrain (2), CPHD may be a manifestation of a severely truncated WDR11 protein. In this context, the menstrual irregularity in the mother of patient 26 may also be ascribed to pituitary dysfunction due to the *WDR11* mutation, although endocrine evaluation was not performed for the mother.

The present study provides a model of molecular diagnosis of genetically heterogeneous disorders. Comparative genomic hybridization and next-generation sequencing identified several pathogenic mutations/deletions in our patients. Identification of the genetic factors underlying diseases is beneficial in the prediction of disease outcomes and possible complications. Furthermore, the molecular diagnosis of each patient serves to improve the accuracy of genetic counseling for the family. For example, mutations in *SOX3* are known to lead to familial HH in an X-linked manner, whereas deletions involving *FGFR1* are inherited in an autosomal dominant manner. In addition, genome-wide copy number analysis is useful for the characterization of contiguous gene deletion syndromes.

This study has implications for future research. Despite systematic molecular analyses, pathogenic abnormalities were not identified in approximately 75% of our patients. These findings are consistent with previous reports from Europe and United States in which monoallelic and biallelic mutations were detected in less than 50% of patients with HH (3, 10, 11, 35), and imply that defects in unexamined genes are present in a significant percentage of patients with HH. For example, mutations in *FGF17*, *IL17RD*, *DUSP6*, *SPRY4*, and *FLRT3*, which have recently been reported as HH causative genes (35), may be hidden in our patients. Furthermore, certain environmental factors may underlie HH, because endocrine-disrupting chemicals have been shown to affect gonadotropin secretion (36). Further studies are necessary to identify novel genes and environmental factors involved in HH. Identification of these genes and factors will clarify the precise regulatory mechanisms of gonadotropin secretion in humans, leading to the development of new therapeutic options for HH.

In summary, genome-wide copy number analysis and systematic mutation screening of 29 genes identified pathogenic defects in 14 of 58 patients with HH. The present study provides a model of molecular diagnosis of genetically heterogeneous conditions. Our results imply that molecular abnormalities in the known causative genes accounts for a relatively small percentage of the genetic causes of HH and that submicroscopic rearrangements encompassing *FGFR1* can lead to IHH as a sole clinical feature. In addition, this study indicates for the first time that polyalanine deletions in *SOX3* and mutations in *WDR11* constitute rare genetic causes of IHH and CPHD, respectively. Further studies, including molecular analysis of large patient groups of various ethnicities and identification of novel causative genes/factors of HH, will serve to advance our understanding of the etiology of HH.

Acknowledgments: The authors appreciate patients and families for participating in the study. The authors thank the following clinicians for providing the samples and information of the patients: Drs. Katsuya Aizu (Saitama Children's Medical Center), Hiroshi Arimura (Kagoshima University), Katsunori Asai (Kobe City Medical Center General Hospital), Hiroyuki Iuchi (Jikei University), Tomohiro Ishii (Keio University), Yoshiki Ueno (Komatsu Municipal Hospital), Akira Ohtake (Saitama Medical University), Kenichi Kashimada (Tokyo Medical and Dental University), Reina Kawarabayashi (Osaka City University), Junko Kanno (Tohoku University), Yoshitomo Kobori (Koshigaya Hospital, Dokkyo Medical University), Yume Suzuki (Jichi Medical University), Sumito Dateki (Nagasaki University), Keisuke Nagasaki (Niigata University), Akie Nakamura (Hokkaido University), Atsushi Nishiyama (Kakogawa West City Hospital), Chikahiko Numakura (Yamagata University), Reiji Hirano (Yamaguchi-ken Saiseikai Shimonoseki General Hospital), Hiroyo Mabe (Kumamoto University), Junko Nishioka (Kurume University), Yoko Miyoshi (Osaka University), Masaaki Yamamoto (Nippon Medical School), and Aya Yoshihara (Toho University Medical Center Omori Hospital).

REFERENCES

1. Bonomi M, Libri DV, Guizzardi F, Guarducci E, Maiolo E, Pignatti E, et al. New understandings of the genetic basis of isolated idiopathic central hypogonadism. Asian J Androl 2012;14:49–56.
2. Raivio T, Avbelj M, McCabe MJ, Romero CJ, Dwyer AA, Tommiska J, et al. Genetic overlap in Kallmann syndrome, combined pituitary hormone deficiency, and septo-optic dysplasia. J Clin Endocrinol Metab 2012;97:E694–9.
3. Dode C, Hardelin JP. Clinical genetics of Kallmann syndrome. Ann Endocrinol (Paris) 2010;71:149–57.
4. Aminzadeh M, Kim HG, Layman LC, Cheetham TD. Rarer syndromes characterized by hypogonadotropic hypogonadism. Front Horm Res 2010;39:154–67.
5. Rapaport R. Disorders of the gonads. In: Kliegman RM, Behrman RE, Jenson HB, Stanton BF, editors. Nelson textbook of pediatrics. 18th ed. Philadelphia: Saunders; 2007:2374–403.
6. Layman LC. Clinical genetic testing for Kallmann syndrome. J Clin Endocrinol Metab 2013;98:1860–2.
7. Beate K, Joseph N, de Nicolas R, Wolfram K. Genetics of isolated hypogonadotropic hypogonadism: role of GnRH receptor and other genes. Int J Endocrinol 2012;2012:147893.
8. Layman LC. The genetic basis of female reproductive disorders: etiology and clinical testing. Mol Cell Endocrinol 2013;370:138–48.
9. Pitteloud N, Quinton R, Pearce S, Raivio T, Acierno J, Dwyer A, et al. Digenic mutations account for variable phenotypes in idiopathic hypogonadotropic hypogonadism. J Clin Invest 2007;117:457–63.
10. Quaynor SD, Kim HG, Cappello EM, Williams T, Chorich LP, Bick DP, et al. The prevalence of digenic mutations in patients with normosmic

hypogonadotropic hypogonadism and Kallmann syndrome. Fertil Steril 2011;96:1424–30.e6.
11. Sykiotis GP, Plummer L, Hughes VA, Au M, Durrani S, Nayak-Young S, et al. Oligogenic basis of isolated gonadotropin-releasing hormone deficiency. Proc Natl Acad Sci U S A 2010;107:15140–4.
12. Kim HG, Ahn JW, Kurth I, Ullmann R, Kim HT, Kulharya A, et al. WDR11, a WD protein that interacts with transcription factor EMX1, is mutated in idiopathic hypogonadotropic hypogonadism and Kallmann syndrome. Am J Hum Genet 2010;87:465–79.
13. Woods KS, Cundall M, Turton J, Rizotti K, Mehta A, Palmer R, et al. Over- and underdosage of SOX3 is associated with infundibular hypoplasia and hypopituitarism. Am J Hum Genet 2005;76:833–49.
14. Alatzoglou KS, Kelberman D, Cowell CT, Palmer R, Arnhold IJ, Melo ME, et al. Increased transactivation associated with SOX3 polyalanine tract deletion in a patient with hypopituitarism. J Clin Endocrinol Metab 2011;96: E685–90.
15. Laumonnier F, Ronce N, Hamel BC, Thomas P, Lespinasse J, Raynaud M, et al. Transcription factor SOX3 is involved in X-linked mental retardation with growth hormone deficiency. Am J Hum Genet 2002;71:1450–5.
16. Takagi M, Ishii T, Torii C, Kosaki K, Hasegawa T. A novel mutation in SOX3 polyalanine tract: a case of kabuki syndrome with combined pituitary hormone deficiency harboring double mutations in MLL2 and SOX3. Pituitary. In press.
17. Pedersen-White JR, Chorich LP, Bick DP, Sherins RJ, Layman LC. The prevalence of intragenic deletions in patients with idiopathic hypogonadotropic hypogonadism and Kallmann syndrome. Mol Hum Reprod 2008;14: 367–70.
18. De Roux N, Genin E, Carel JC, Matsuda F, Chaussain JL, Milgrom E. Hypogonadotropic hypogonadism due to loss of function of the KiSS1-derived peptide receptor GPR54. Proc Natl Acad Sci U S A 2003;100:10972–6.
19. Klopocki E, Fiebig B, Robinson P, Tonnies H, Erdogan F, Ropers HH, et al. A novel 8 Mb interstitial deletion of chromosome 8p12-p21.2. Am J Med Genet A 2006;140:873–7.
20. Wincent J, Schulze A, Schoumans J. Detection of CHD7 deletions by MLPA in CHARGE syndrome patients with a less typical phenotype. Eur J Med Genet 2009;52:271–2.
21. Trarbach EB, Teles MG, Costa EM, Abreu AP, Garmes HM, Guerra G Jr, et al. Screening of autosomal gene deletions in patients with hypogonadotropic hypogonadism using multiplex ligation-dependent probe amplification: detection of a hemizygosis for the fibroblast growth factor receptor 1. Clin Endocrinol (Oxf) 2010;72:371–6.
22. Miya K, Shimojima K, Sugawara M, Shimada S, Tsuri H, Harai-Tanaka T, et al. A de novo interstitial deletion of 8p11.2 including ANK1 identified in a patient with spherocytosis, psychomotor developmental delay, and distinctive facial features. Gene 2012;506:146–9.
23. Fukami M, Iso M, Sato N, Igarashi M, Seo M, Kazukawa I, et al. Submicroscopic deletion involving the fibroblast growth factor receptor 1 gene in a patient with combined pituitary hormone deficiency. Endocr J 2013;60: 1013–20.
24. Young J, Metay C, Bouligand J, Tou B, Francou B, Maione L, et al. SEMA3A deletion in a family with Kallmann syndrome validates the role of semaphorin 3A in human puberty and olfactory system development. Hum Reprod 2012;27:1460–5.
25. Dateki S, Fukami M, Uematsu A, Kaji M, Iso M, Ono M, et al. Mutation and gene copy number analyses of six pituitary transcription factor genes in 71 patients with combined pituitary hormone deficiency: identification of a single patient with LHX4 deletion. J Clin Endocrinol Metab 2010;95:4043–7.
26. Suzuki E, Yatsuga S, Igarashi M, Miyado M, Nakabayashi K, Hayashi K, et al. De novo frameshift mutation in fibroblast growth factor 8 in a male patient with gonadotropin deficiency. Horm Res Paediatr 2014;81:139–44.
27. Cooper GM, Coe BP, Girirajan S, Rosenfeld JA, Vu TH, Baker C, et al. A copy number variation morbidity map of developmental delay. Nat Genet 2011; 43:838–46.
28. Gorbenko Del Blanco D, Romero CJ, Diaczok D, de Graaff LC, Radovick S, Hokken-Koelega AC. A novel OTX2 mutation in a patient with combined pituitary hormone deficiency, pituitary malformation, and an underdeveloped left optic nerve. Eur J Endocrinol 2012;167:441–52.
29. Turton JP, Strom M, Langham S, Dattani MT, Le Tissier P. Two novel mutations in the POU1F1 gene generate null alleles through different mechanisms leading to combined pituitary hormone deficiency. Clin Endocrinol (Oxf) 2012;76:387–93.
30. Kelberman D, Dattani MT. Hypopituitarism oddities: congenital causes. Horm Res 2007;68(Suppl 5):138–44.
31. Wang Y, Jiang F, Zhuo Z, Wu XH, Wu YD. A method for WD40 repeat detection and secondary structure prediction. PLoS One 2013;8:e65705.
32. Wu XH, Wang Y, Zhuo Z, Jiang F, Wu YD. Identifying the hotspots on the top faces of WD40-repeat proteins from their primary sequences by beta-bulges and DHSW tetrads. PLoS One 2012;7:e43005.
33. Yu S, Fiedler S, Stegner A, Graf WD. Genomic profile of copy number variants on the short arm of human chromosome 8. Eur J Hum Genet 2010;18: 1114–20.
34. Schwarting GA, Wierman ME, Tobet SA. Gonadotropin-releasing hormone neuronal migration. Semin Reprod Med 2007;25:305–12.
35. Miraoui H, Dwyer AA, Sykiotis GP, Plummer L, Chung W, Feng B, et al. Mutations in FGF17, IL17RD, DUSP6, SPRY4, and FLRT3 are identified in individuals with congenital hypogonadotropic hypogonadism. Am J Hum Genet 2013;92:725–43.
36. Mueller JK, Heger S. Endocrine disrupting chemicals affect the Gonadotropin releasing hormone neuronal network. Reprod Toxicol 2014;44: 73–84.

SUPPLEMENTAL TABLE 1

Patients participating in the present study.

Patient no.	Age at diagnosis (y)	Clinical diagnosis	Family history	Additional clinical feature	Testes volume (ml)
Male					
1	13	nIHH			1.0
2	15	nIHH	Father: delayed puberty		1.5
3	17	nIHH			No data
4	18	nIHH			No data
5	15	nIHH			No data
6	17	nIHH			No data
7	18	nIHH			2.0
8	18	nIHH			0.5
9	34	nIHH			No data
10	No data	nIHH			No data
11	13	KS	Brother: KS		Small
12	16	KS		Cleft lip and plate, MR	No data
13	16	KS		Cleft lip and plate, hearing loss, VSD, MR	>1.0
14	25	KS			No data
15	13	KS			3.0
16	7	KS			No data
17	7	KS			No data
18	20	KS			No data
19	21	KS			2.0
20	21	KS	Sister: delayed puberty	Cleft lip and plate, ASD	Small
21	40	KS	Brother: KS		No data
22	38	KS	Brother: KS		No data
23	45	KS	Brother: KS	Synkinesis, renal agenesis, persistent olfactory artery aneurysm, obesity	No data
24	10	KS			No data
25	28	KS			3.0
26	2	CPHD		MR, obesity	2.0
27	0	CPHD			No data
28	5	CPHD			No data
29	16	CHARGE		Tetralogy of Fallot, hearing loss, cleft lip and plate	No data
30	2	SOD	Brother: cleft plate, hypothyroidism	Microphthalmia, optic atrophy	No data
31	13	SOD			No data
32	1.2	IHH			No data
33	14	IHH			No data
34	No data	IHH			No data
Female					
35	22	nIHH			–
36	22	nIHH			–
37	1	nIHH			–
38	20	nIHH			–
39	14	nIHH			–
40	16	nIHH			–
41	17	nIHH			–
42	27	nIHH			–
43	28	nIHH			–
44	15	nIHH			–
45	27	nIHH			–
46	56	KS			–
47	9	KS			–
48	14	KS			–
49	15	KS			–
50	29	KS			–
51	No data	KS			–
52	0.2	CPHD		Cleft lip and plate, hypoplastic nasal septum	–
53	2	CHARGE			–
54	12	CHARGE			–
55	16	CHARGE		Microphthalmia, choroidal coloboma	–
56	No data	IHH			–
57	16	IHH		Hearing loss	–
58	No data	IHH			–

Note: ASD = atral septal defect; CHARGE = CHARGE syndrome; CPHD = combined pituitary hormone deficiency; F = female; nIHH = normosmic isolated hypogonadotropic hypogonadism; IHH = isolated hypogonadotropic hypogonadism with unknown olfactory function; KS = Kallmann syndrome; M = male; MR = mental retardation; SOD = septo-optic dysplasia; VSD = ventricular septal defect.

Izumi. Genetic basis of gonadotropin deficiency. Fertil Steril 2014.

SUPPLEMENTAL TABLE 2

Genes and pseudogenes involved in the deletion.

Gene symbol (Refseq)	Accession no.	Description
UNC5D	NM_080872	unc-5 homologue D (*C. elegans*)
KCNU1	NM_001031836	Potassium channel, subfamily U, member 1
ZNF703	NM_025069	Zinc finger protein 703
ERLIN2	NM_007175	ER lipid raft associated 2
LOC728024	NR_003671	chromosome X open reading frame 56 pseudogene
PROSC	NM_007198	proline synthetase co-transcribed homolog (bacterial)
GPR124	NM_032777	G protein-coupled receptor 124
BRF2	NM_018310	BRF2, RNA polymerase III transcription initiation factor 50 kDa subunit
RAB11FIP1	NM_025151	RAB11 family interacting protein 1 (class I)
GOT1L1	NM_152413	glutamic-oxaloacetic transaminase 1-like 1
ADRB3	NM_000025	adrenoceptor beta 3
EIF4EBP1	NM_004095	eukaryotic translation initiation factor 4E binding protein 1
ASH2L	NM_004674	ash2 (absent, small, or homeotic)-like (*Drosophila*)
STAR	NM_000349	steroidogenic acute regulatory protein
LSM1	NM_014462	LSM1 homologue, U6 small nuclear RNA associated (*S. cerevisiae*)
BAG4	NM_004874	BCL2-associated athanogene 4
DDHD2	NM_001164232	DDHD domain containing 2
PPAPDC1B	NM_001102559	phosphatidic acid phosphatase type 2 domain containing 1B
WHSC1L1	NM_017778	Wolf-Hirschhorn syndrome candidate 1-like 1
LETM2	NM_001199659	leucine zipper-EF-hand containing transmembrane protein 2
FGFR1	NM_001174063	fibroblast growth factor receptor 1
C8orf86	NM_207412	chromosome 8 open reading frame 86
RNF5P1	NR_003129	ring finger protein 5, E3 ubiquitin protein ligase pseudogene 1
TACC1	NM_001122824	transforming, acidic coiled-coil containing protein 1
PLEKHA2	NM_021623	pleckstrin homology domain containing, family A (phosphoinositide-binding specific) member 2
HTRA4	NM_153692	HtrA serine peptidase 4
TM2D2	NM_001024380	TM2 domain containing 2
ADAM9	NM_003816	ADAM metallopeptidase domain 9
ADAM32	NM_145004	ADAM metallopeptidase domain 32
ADAM5	NM_001040073	ADAM metallopeptidase domain 5, pseudogene

Izumi. Genetic basis of gonadotropin deficiency. Fertil Steril 2014.

SUPPLEMENTAL TABLE 3

Allele frequency of rare polymorphisms.

Gene	Polymorphism	dbSNP ID	Allele frequency in our patients	Allele frequency in the Japanese general population[a]	Statistical significance (*P* value)
WDR11	p.A1076T	rs200126172	1/116	18/2,286	.9294
LHB	p.R88W	rs146251380	1/116	4/1,434	.2867
LHB	p.Y57H	rs371722800	3/116	No data	No data
LHX3	p.R208C	rs146251380	1/116	4/1,434	.2867
LHX3	p.A322T	rs201356862	1/116	13/2,000	.7842
PROKR2	p.Y113H	rs202203360	1/116	4/2,204	.1234
PROKR2	p.W178S	rs201835496	1/116	1/76	.762

[a] Based on the Human Genetic Variation Browser.

Izumi. Genetic basis of gonadotropin deficiency. Fertil Steril 2014.

Genome-wide parent-of-origin DNA methylation analysis reveals the intricacies of human imprinting and suggests a germline methylation-independent mechanism of establishment

Franck Court,[1,15] Chiharu Tayama,[2,15] Valeria Romanelli,[1,15] Alex Martin-Trujillo,[1,15] Isabel Iglesias-Platas,[3] Kohji Okamura,[4] Naoko Sugahara,[2] Carlos Simón,[5] Harry Moore,[6] Julie V. Harness,[7] Hans Keirstead,[7] Jose Vicente Sanchez-Mut,[8] Eisuke Kaneki,[9] Pablo Lapunzina,[10] Hidenobu Soejima,[11] Norio Wake,[9] Manel Esteller,[8,12,13] Tsutomu Ogata,[14] Kenichiro Hata,[2] Kazuhiko Nakabayashi,[2,16,17] and David Monk[1,16,17]

[1–14] *[Author affiliations appear at the end of the paper.]*

Differential methylation between the two alleles of a gene has been observed in imprinted regions, where the methylation of one allele occurs on a parent-of-origin basis, the inactive X-chromosome in females, and at those loci whose methylation is driven by genetic variants. We have extensively characterized imprinted methylation in a substantial range of normal human tissues, reciprocal genome-wide uniparental disomies, and hydatidiform moles, using a combination of whole-genome bisulfite sequencing and high-density methylation microarrays. This approach allowed us to define methylation profiles at known imprinted domains at base-pair resolution, as well as to identify 21 novel loci harboring parent-of-origin methylation, 15 of which are restricted to the placenta. We observe that the extent of imprinted differentially methylated regions (DMRs) is extremely similar between tissues, with the exception of the placenta. This extra-embryonic tissue often adopts a different methylation profile compared to somatic tissues. Further, we profiled all imprinted DMRs in sperm and embryonic stem cells derived from parthenogenetically activated oocytes, individual blastomeres, and blastocysts, in order to identify primary DMRs and reveal the extent of reprogramming during preimplantation development. Intriguingly, we find that in contrast to ubiquitous imprints, the majority of placenta-specific imprinted DMRs are unmethylated in sperm and all human embryonic stem cells. Therefore, placental-specific imprinting provides evidence for an inheritable epigenetic state that is independent of DNA methylation and the existence of a novel imprinting mechanism at these loci.

[Supplemental material is available for this article.]

Genomic imprinting is a form of epigenetic regulation that results in the expression of either the maternally or paternally inherited allele of a subset of genes (Ramowitz and Bartolomei 2011). This imprinted expression of transcripts is crucial for normal mammalian development. In humans, loss-of-imprinting of specific loci results in a number of diseases exemplified by the reciprocal growth phenotypes of the Beckwith-Wiedemann and Silver-Russell syndromes, and the behavioral disorders Angelman and Prader-Willi syndromes (Kagami et al. 2008; Buiting 2010; Choufani et al. 2010; Eggermann 2010; Kelsey 2010; Mackay and Temple 2010). In addition, aberrant imprinting also contributes to multigenic disorders associated with various complex traits and cancer (Kong et al. 2009; Monk 2010).

Imprinted loci contain differentially methylated regions (DMRs) where cytosine methylation marks one of the parental alleles, providing *cis*-acting regulatory elements that influence the allelic expression of surrounding genes. Some DMRs acquire their allelic methylation during gametogenesis, when the two parental genomes are separated, resulting from the cooperation of the de novo methyltransferase DNMT3A and its cofactor DNMT3L (Bourc'his et al. 2001; Hata et al. 2002). These primary, or germline imprinted DMRs are stably maintained throughout somatic development, surviving the epigenetic reprogramming at the oocyte-to-embryo transition (Smallwood et al. 2011; Smith et al. 2012). To confirm that an imprinted DMR functions as an imprinting control region (ICR), disruption of the imprinted expression upon genetic deletion of that DMR, either through experimental targeting in mouse or that which occurs spontaneously in humans, is required. A subset of DMRs, known as secondary DMRs, acquire methylation during development and are regulated by nearby germline DMRs in a hierarchical fashion (Coombes et al. 2003; Lopes et al. 2003; Kagami et al. 2010).

[15] These authors contributed equally to this work.
[16] These authors jointly directed this work.
[17] Corresponding authors
E-mail nakabaya-k@ncchd.go.jp
E-mail dmonk@idibell.cat
Article published online before print. Article, supplemental material, and publication date are at http://www.genome.org/cgi/doi/10.1101/gr.164913.113.

24:554–569 Published by Cold Spring Harbor Laboratory Press; ISSN 1088-9051/14; www.genome.org

With the advent of large-scale, base-resolution methylation technologies, it is now possible to discriminate allelic methylation dictated by sequence variants from imprinted methylation. Yet our knowledge of the total number of imprinted DMRs in humans, and their developmental dynamics, remains incomplete, hampered by genetic heterogeneity of human samples.

Here we present high-resolution mapping of human imprinted methylation. We performed whole-genome-wide bisulfite sequencing (WGBS) on leukocyte-, brain-, liver-, and placenta-derived DNA samples to identify partially methylated regions common to all tissues consistent with imprinted DMRs. We subsequently confirmed the partial methylated states in tissues using high-density methylation microarrays. The parental origin of methylation was determined by comparing microarray data for DNA samples from reciprocal genome-wide uniparental disomy (UPD) samples, in which all chromosomes are inherited from one parent (Lapunzina and Monk 2011), and androgenetic hydatidiform moles, which are created by the fertilization of an oocyte lacking a nucleus by a sperm that endoreduplicates. The use of uniparental disomies and hydatidiform moles meant that our analyses were not subjected to genotype influences, enabling us to characterize all known imprinted DMRs at base-pair resolution and to identify 21 imprinted domains, which we show are absent in mice. Lastly, we extended our analyses to determine the methylation profiles of all imprinted DMRs in sperm, stem cells derived from parthenogenetically activated metaphase-2 oocyte blastocytes (phES) (Mai et al. 2007; Harness et al. 2011), and stem cells (hES) generated from both six-cell blastomeres and the inner cell mass of blastocysts, delineating the extent of embryonic reprogramming that occurs at these loci during human development.

Results

Characterization of parent-of-origin methylation profiles in human tissues using high-resolution approaches

We combined whole-genome bisulfite sequencing with Illumina Infinium HumanMethylation 450K BeadChip arrays to generate methylation profiles. To validate this approach, we compared the DNA methylation profiles generated by each method. Methylation scores produced by the two methods are very similar when the same DNA samples were assessed by both techniques (linear regression WGBS vs. Infinium array: leukocytes $R^2 = 0.92$; brain $R^2 = 0.91$; placenta $R^2 = 0.92$) (Supplemental Fig. S1). To determine the similarity between normal biparental leukocytes and those from reciprocal genome-wide UPDs, we compared the methylation values obtained from the Infinium array. This revealed high correlations between samples, indicating that the DNAs were similar, differing only at imprinted loci (linear regression: leukocytes vs. leukocytes $R^2 = 0.95$–0.98; mean control leukocytes vs. mean pUPD $R^2 = 0.98$; mean control leukocytes vs. mUPD $R^2 = 0.98$; mUPD vs. mean pUPD $R^2 = 0.97$; F-statistics $P < 0.001$).

Before we attempted to discover novel imprinted DMRs in the human genome, we wished to determine the effectiveness of the Infinium array to identify known imprinted DMRs. Loci were identified which contained at least three Infinium probes with an average minimal difference of 0.3 β-values (absolute methylation difference >30%) between reciprocal genome-wide UPD leukocyte samples, and with a prerequisite that the β-values for normal leukocytes should be between these extremes. Using these criteria, we identified 818 windows that could be merged into 145 regions harboring 576 probes incorporating 30 known DMRs within 25 imprinted domains (Table 1; Fig. 1A) (Limma linear model $P < 0.05$), and presented an intermediate methylation profile in all somatic tissues (Fig. 1B). The only imprinted DMRs not found using this approach were the IG-DMR located between *MEG3* and *DLK1* on chromosome 14, as this region does not have probes on this array platform and *IGF2*-DMR0 only contains a single probe.

Identification of new DMRs within known imprinted domains

In addition to the known imprinted DMRs, the Infinium array screen of reciprocal UPDs and tissues samples uncovered several previously unidentified DMRs located within existing imprinted domains. We discovered four maternally methylated CpG islands located between the *SNRPN* and *NDN* genes on chromosome 15, a region associated with the Angelman and Prader-Willi syndromes. The methylation profiles at the *SNRPN*, *NDN*, and *MAGEL2* promoters are well-established (El-Maarri et al. 2001; Sharp et al. 2010). However, little is known about the intervening ~1-Mb gene-poor region, which is likely to have arisen from an ancient duplication event, since these novel DMRs share 97.8% sequence identity with additional CpG-rich regions in the interval. We confirm the maternal methylation at these four regions using bisulfite PCR and sequencing, incorporating heterozygous SNPs in brain and leukocyte DNA (Supplemental Fig. S2A). Further analysis of this region revealed that the promoter region for *MKRN3* and *MIR4508* are also differentially methylated.

Extending our analysis to imprinted domains on other autosomes, we identified an ~600-bp interval of maternal methylation 4 kb 3′ from the *ZNF597* gene (Fig. 1C). Although the promoter of *ZNF597* is a paternally methylated bidirectional silencer presumably responsible for regulating the imprinted expression of both *ZNF597* and *NAA60* (previously known as *NAT15*), this region is unlikely to be the ICR for the domain as its methylation is somatically acquired (Nakabayashi et al. 2011). In addition, WGBS and Infinium array data sets revealed a maternally methylated DMR within intron 2 of *MEG8* within the chromosome 14 imprinted domain (Supplemental Fig. S2B). Lastly, we identify two maternally methylated regions. The first is an ~1-kb CpG island overlapping the promoter of isoform 3 of the *ZNF331* gene, and the second coincides with exon 2 of *DIRAS3* (Supplemental Fig. S2C).

Genome-wide methylation profiling identifies novel imprinted domains

To determine if there are additional imprinted DMRs in the human genome, we screened for regions of intermediate methylation common to lymphocyte, brain, and liver WGBS data sets. Using a sliding window approach that takes into account 25 consecutive CpG sites and following removal of class 1 transposable elements (LINEs, *Alu*/SINEs, and LTR elements) and satellite DNA, we identified 356 nonoverlapping, single-copy regions in pairwise comparisons of tissues, of which 63 loci were common to the all tissues ($0.25 < \text{mean} \pm 1.5\ \text{SD} < 0.75$) (Fig. 2A; Supplemental Table S1).

A screen for three consecutive partially methylated probes in leukocyte, brain, liver, kidney, and muscle Infinium data sets, with a profile consistent with parent-of-origin methylation in the reciprocal UPD leukocyte samples, identified 116 regions (Supplemental Table S1). By combining the 356 regions detected by WGBS and the 116 loci identified by the Infinium array, we identified 64 regions in common, which included all known imprinted DMRs and 17 CpG-rich sequences possessing a methylation profile consistent with imprinting. Using standard bisulfite PCR, we assessed

Table 1. Location of parent-of-origin methylation identified in this study

Known imprinted DMRs ($n = 36$)								Novel DMRs ($n = 25$)							
								Novel DMRs near known imprinted loci ($n = 8$)							
		Extent (WGBS)							Extent (WGBS)						
Gene locus	Chr	Start	Finish	# Infinium probes	GC content	# CpG	Methylation origin	Gene locus	Chr	Start	Finish	# Infinium probes	GC Content	# CpG	Methylation origin
DIRAS3	1	68515433	68517545	17	0.50	88	M	*DIRAS3* Ex2	1	68512505	68513486	8	0.52	39	M
ZDBF2	2	207114583	207136544	8	0.45	439	P	*MEG8*	14	101370741	101371419	1	0.66	43	M
NAP1L5	4	89618184	89619237	15	0.57	57	M	*SNRPN* intragenic CpG32	15	24346736	24347142	1	0.59	30	M
FAM50B	6	3849082	3850359	25	0.65	90	M	*SNRPN* intragenic CpG29	15	24671872	24672679	4	0.59	39	M
PLAGL1	6	144328078	144329888	16	0.58	143	M	*SNRPN* intragenic CpG30	15	24722753	24723071	1	0.66	29	M
IGF2R	6	160426558	160427561	2	0.70	74	M	*SNRPN* intragenic CpG40	15	25017924	25018886	4	0.51	67	M
GRB10	7	50848726	50851312	9	0.60	171	M	*ZNF597*	16	3481801	3482388	2	0.54	29	M
PEG10	7	94285537	94287960	53	0.60	119	M	*ZNF331*	19	54057086	54058425	4	0.66	102	M
MEST	7	130130122	130134388	55	0.54	226	M								
TRAPPC9	8	141108147	141111081	8	0.62	193	M	Novel DMRs ($n = 6$)							
INPP5F	10	121578046	121578727	4	0.59	52	M	*PPIEL*	1	40024626	40025540	4	0.54	39	M
H19	11	2018812	2024740	48	0.60	250	P	*WDR27*	6	170054504	170055618	2	0.56	58	M
IGF2 DMR2	11	2153991	2155112	9	0.65	63	P	*HTR5A*	7	154862719	154863382	6	0.62	55	M
IGF2 DMR0	11	2168333	2169768	1	0.62	33	P	*CXORF56 pseudogene/ ERLIN2*	8	37604992	37606088	7	0.45	37	M
KvDMR1	11	2719948	2722259	30	0.67	192	M	*WRB*	21	40757510	40758276	4	0.61	43	M
RB1	13	48892341	48895763	12	0.59	195	M	*NHP2L1*	22	42077774	42078873	8	0.54	63	M
IG-DMR	14	101275427	101278058	0	0.52	64	P								
MEG3	14	101290524	101293978	33	0.60	188	P	Known imprinted DMRs ($n = 2$) & novel DMRs ($n = 15$)							
MKRN3/ MIR4508	15	23807086	23812495	12	0.44	109	M	Placental-specific DMRs ($n = 17$)							
MAGEL2	15	23892425	23894029	6	0.55	51	M	*GPR1-AS*	2	207066967	207069445	3	0.49	86	M
NDN	15	23931451	23932759	8	0.65	108	M	*MCCC1*	3	182815725	182817627	13	0.54	94	M
SNRPN	15	25068564	25069481	8	0.42	19	M	*PDE4D*	5	58333774	58336554	7	0.54	145	M
SNRPN	15	25093008	25093829	4	0.49	44	M	*LIN28B*	6	105400631	105402559	8	0.45	62	M
SNRPN	15	25123027	25123905	5	0.47	45	M	*AIM1*	6	106957945	106961974	19	0.54	203	M
SNURF	15	25200004	25201976	7	0.60	113	M	*AGBL3*	7	134671024	134672011	12	0.59	74	M
IGF1R	15	99408496	99409650	7	0.51	55	M	*ZFAT*	8	135707227	135710114	3	0.60	111	M
ZNF597/ NAA60	16	3492828	3494463	11	0.54	76	P	*GLIS3*	9	4297279	4300182	9	0.63	235	M
ZNF331	19	54040510	54042212	11	0.64	125	M	*DCAF10*	9	37800140	37802937	5	0.56	157	M
PEG3	19	57348493	57353271	36	0.59	221	M	*FAM196A/DOCK1*	10	128993405	128995242	10	0.72	198	M
MCTS2P/HM13	20	30134663	30135933	9	0.48	47	M	*ZC3H12C*	11	109962727	109964784	9	0.66	198	M
BLCAP/NNAT	20	36148604	36150528	35	0.55	135	M	*N4BP2L1*	13	33000694	33002448	13	0.66	136	M
L3MBTL	20	42142365	42144040	25	0.65	84	M	*RGMA*	15	93614998	93616859	8	0.61	134	M
GNAS	20	57414039	57418612	23	0.57	257	P	*FAM20A*	17	66596155	66597643	4	0.72	162	M
NESP-AS/ GNAS-AS1	20	57425649	57428033	62	0.61	128	M	*ZNF396*	18	32956510	32957580	9	0.64	86	M
GNAS XL	20	57428905	57431463	6	0.65	200	M	*MIR512-1* cluster	19	54150515	54155608	6	0.53	216	M
GNAS Ex1A	20	57463265	57465201	38	0.67	198	M	*DNMT1*	19	10303506	10306415	10	0.55	129	M

The extent of imprinted methylation is defined by the size of the intermediately methylated region from the lymphocyte (for ubiquitous DMRs) and placenta (for placental-specific DMRs) WGBS data set.

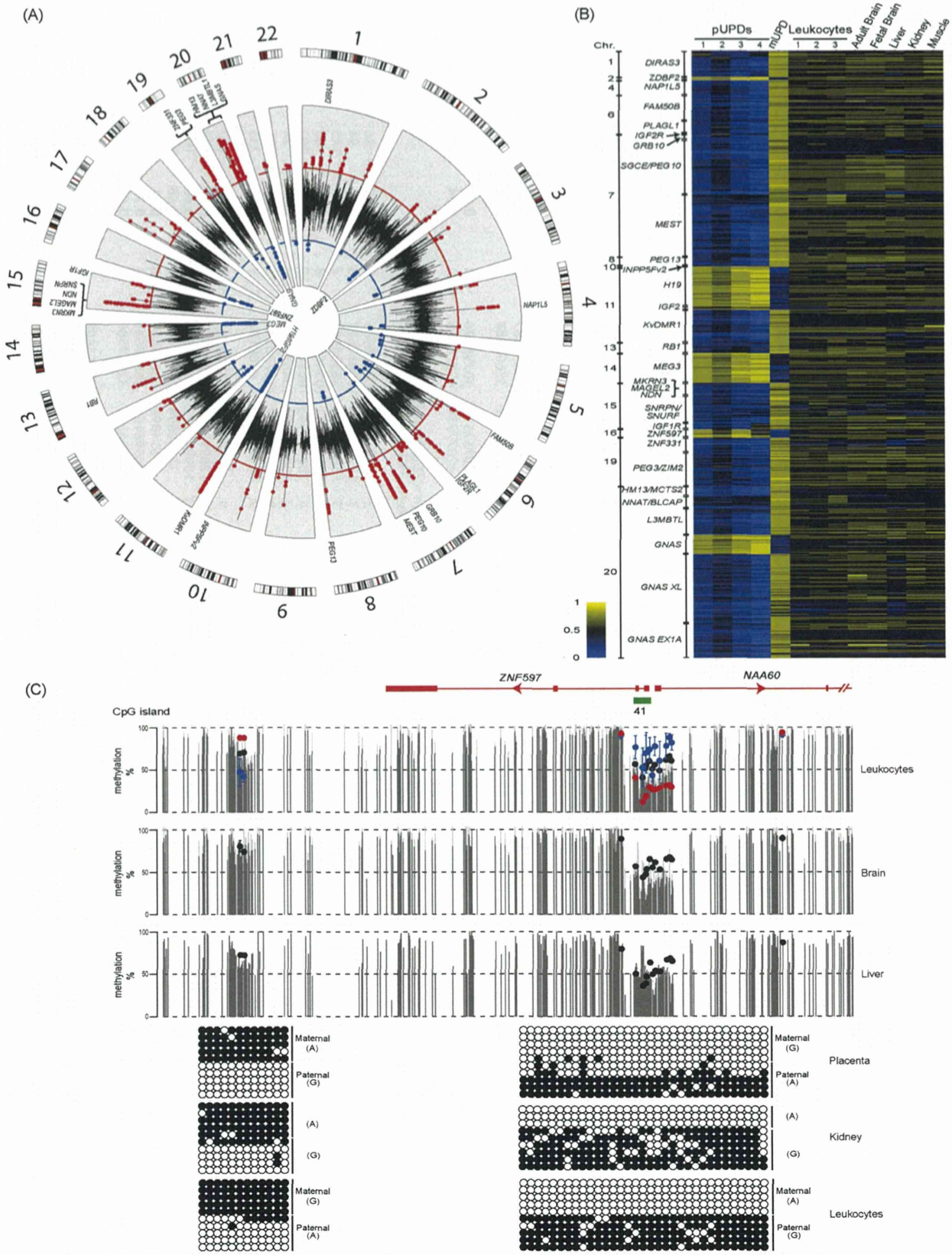

Figure 1. (Legend on next page)